

## Development and Characterization of GaInP/GaAs HBTs for High Voltage Operation

P. Kurpas, F. Brunner, W. Doser\*, A. Maaßdorf, R. Doerner, M. Rudolph, H. Blanck\*, W. Heinrich, and J. Würfl

Ferdinand-Braun-Institut für Höchstfrequenztechnik (FBH)

Albert-Einstein-Str. 11, 12489 Berlin, Germany

Phone: +49-30-6392-2674, fax: +49-30-6392-2685, e-mail: kurpas@fbh-berlin.de

\* United Monolithic Semiconductors GmbH, Wilhelm-Runge-Str. 11, 89081 Ulm, Germany

Phone: +49-731-505-3097, Fax: +49-731-505-3005, e-mail: doser@ums-ulm.de © 2001 GaAs Mantech

### Abstract

This paper reports on the development of GaInP/GaAs HBTs suitable for high-voltage operation. First, the dependence of breakdown voltages on thickness and doping level of the collector layer is determined. High  $BV_{cbo}$  and  $BV_{ceo}$  values of 69 V and 41 V, respectively, are obtained for a 2.8  $\mu\text{m}$  thick collector doped to  $4 \times 10^{15} \text{ cm}^{-3}$ . The required process modifications for this very high device topology are described. The fabricated high-voltage HBTs show DC characteristics comparable to our "standard" low-voltage HBTs. However, a limitation in usable current density becomes visible at higher voltages due to the lack of electrical ballasting and insufficient heat sinking of these devices.  $f_T$  and  $f_{max}$  values of 24 GHz and 50 GHz, respectively, document good RF performance. A comparably small HBT power cell with  $10 \times 3 \times 30 \mu\text{m}^2$  emitter area delivers 2.2 W of microwave power with a high PAE of 66% at 2 GHz and 20 V bias voltage.

### INTRODUCTION

GaAs-based heterojunction bipolar transistors (HBTs) are increasingly used for power applications in mobile communications. Beside the huge market of cellular handsets, which requires highly efficient HBTs operated at low supply voltage, the potential of HBTs is very promising for applications in base station circuits, too. This application requires highly linear HBT power cells, which can be operated at collector-emitter voltages around 25V. Very good performance of HBT-based power cells at bias voltages even higher than 30 V was already reported by Hill et.al. [1]. This work demonstrated impressively the superiority of HBTs for high voltage applications. However, development of such HBTs still remains a challenge.

In this paper we report on GaInP/GaAs HBT power cells, which can be operated at bias voltages up to 20 V. The dependence of base-collector ( $BV_{cbo}$ ) and collector-emitter ( $BV_{ceo}$ ) breakdown voltages on the collector structure are given. Results of DC characterization confirm the high quality of epi-material and processing. Finally, results of on-wafer power measurements from first devices demonstrate good performance although so far without electrical ballasting and heat sinking.

### EXPERIMENTAL

The high voltage HBT structures (HV-HBTs) are grown on 4-inch GaAs substrates in an Aixtron AIX2400 Planetary<sup>TM</sup> MOVPE reactor. The layer structures mainly consist of a 700 nm GaAs subcollector layer ( $n=5 \times 10^{18} \text{ cm}^{-3}$ ), a 2800 nm thick GaAs collector layer (doping variation  $n=4 - 20 \times 10^{15} \text{ cm}^{-3}$ ), a 100 nm GaAs base layer ( $p=4 \times 10^{19} \text{ cm}^{-3}$ ), a 40 nm  $\text{Ga}_{0.51}\text{In}_{0.49}\text{P}$  emitter layer ( $n=5 \times 10^{17} \text{ cm}^{-3}$ ), and GaAs and InGaAs contact layers. Si and C are used for the n-type and p-type doping, respectively. The HBT process technology is based on a two-mesa approach in order to access the base and the collector layers. Device isolation is provided by He-ion implantation through the subcollector layer. The lateral emitter and base definition is based on a selective dry-etching process as already described in detail in [2].  $\text{WSiN}_x/\text{Ti}/\text{Pt}/\text{Au}$ ,  $\text{Ti}/\text{Pt}/\text{Au}$  and  $\text{Ni}/\text{Ge}/\text{Au}/\text{Ni}/\text{Au}$  metal systems are used for the emitter, base and collector contacts, respectively. Interconnections are made by  $\text{Ti}/\text{Pt}/\text{Au}$  metal and emitter thermal shunts are formed by a 20  $\mu\text{m}$  thick electroplated Au layer [2].

For the etching of the thick collector layer, which has three times the thickness as compared with the common low-

voltage HBTs, sulfuric acid is used taking advantage of its superior selectivity against a 20 nm thin GaInP etch-stop layer. However, the control of underetching was a point for optimization of both the resist properties and the layout. After the collector wet-etching the total topology of the HBT device reaches 4  $\mu\text{m}$ . This high topology requires optimized processing to deal with. We found that after only slight adaptations our thick-resist stepper-lithography is able to provide the required resolution. Therefore, it was not necessary to include any planarization. We use only a 300 nm thin  $\text{SiN}_x$  layer for passivation. The 2  $\mu\text{m}$  thick interconnect metal is able to climb the base mesa on its gentle sloped side oriented along the (011) plane as shown in Fig. 1.

HBT single devices with an emitter area of  $3 \times 30 \mu\text{m}^2$  as well as power cells with up to 10 emitter fingers and a total emitter area of  $10 \times 3 \times 30 \mu\text{m}^2$  are fabricated. DC measurements are performed using a commercial wafer mapping system. The power performance is characterized by S-parameter and load-pull measurements at 2 GHz.

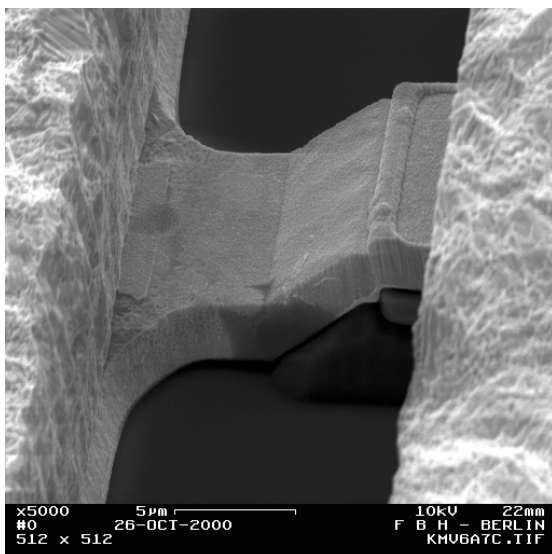


Fig. 1: SEM picture showing the base contact interconnection climbing the 3 $\mu\text{m}$  high base mesa.

## RESULTS

Table I shows the measured collector-base ( $BV_{cbo}$ ) and collector-emitter breakdown voltage ( $BV_{ceo}$ ) of HV-HBTs with 2.8  $\mu\text{m}$  collector thickness and different doping levels in comparison with our "standard" low-voltage HBT (collector: 1.0  $\mu\text{m}$ ,  $2 \times 10^{16} \text{ cm}^{-3}$ ). The increase in breakdown voltage with growing collector thickness and decreasing doping level is confirmed. High breakdown

voltage values  $BV_{cbo}$  up to 70 V and  $BV_{ceo}$  above 40 V are obtained for the lowest collector doping level. These values compare well with results reported in [1].

Fig. 2 presents typical Gummel plots measured for HV-HBTs and for a "standard" HBT. High current gain, low recombination currents and good junction idealities are obtained for HV-HBTs. Fig. 3 shows the output characteristics of HV-HBTs with  $6 \times 10^{15} \text{ cm}^{-3}$  collector doping. At higher current densities ( $> 2.5 \times 10^4 \text{ A/cm}^2$ ) these HV-HBTs are destroyed already at 20 V. However, at current densities well below  $1 \times 10^4 \text{ A/cm}^2$  device operation at voltages higher than 40 V is possible. The strong dependence of the maximum operating voltage on current density is obviously caused by insufficient thermal stabilization and the lack of ballasting for this type of devices.

**TABLE I**  
DEPENDENCE OF COLLECTOR-BASE ( $BV_{cbo}$ ) AND COLLECTOR-EMITTER BREAKDOWN VOLTAGE ( $BV_{ceo}$ ) ON THICKNESS AND DOPING LEVEL OF COLLECTOR LAYER

| collector layer                |                                | breakdown voltage |                   |
|--------------------------------|--------------------------------|-------------------|-------------------|
| thickness<br>( $\mu\text{m}$ ) | doping<br>( $\text{cm}^{-3}$ ) | $BV_{cbo}$<br>(V) | $BV_{ceo}$<br>(V) |
| 1.0                            | $2 \times 10^{16}$             | 28                | 13                |
| 2.8                            | $2 \times 10^{16}$             | 40                | 18                |
| 2.8                            | $8 \times 10^{15}$             | 54                | 26                |
| 2.8                            | $6 \times 10^{15}$             | 63                | 33                |
| 2.8                            | $4 \times 10^{15}$             | 69                | 41                |

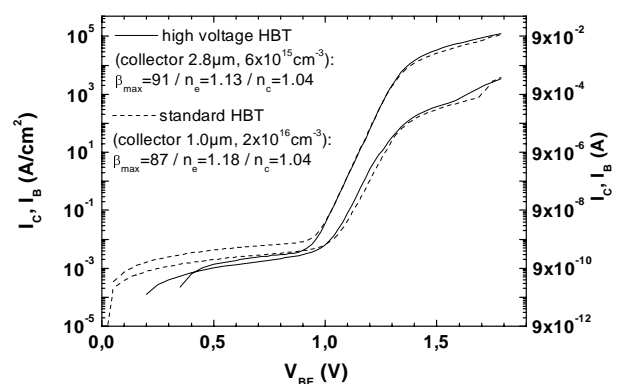


Fig. 2: Comparison of Gummel plots obtained for high voltage HBT and low voltage "standard" HBT ( $1 \times 3 \times 30 \mu\text{m}^2$ ).

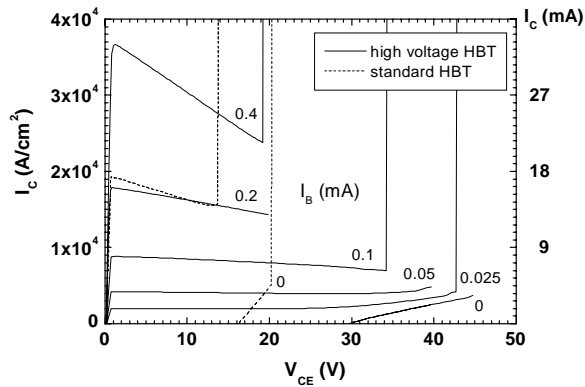


Fig. 3 Output characteristics of high voltage and "standard" HBTs. Destruction of devices is visible after critical  $I_c$  and  $V_{ce}$  is reached.

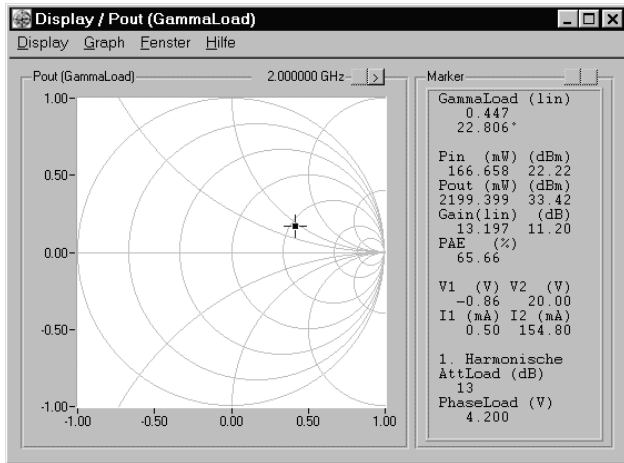


Fig. 4: On-wafer power measurements at 20 V bias voltage and 2 GHz for a  $10 \times 3 \times 30 \mu\text{m}^2$  HBT power cell.

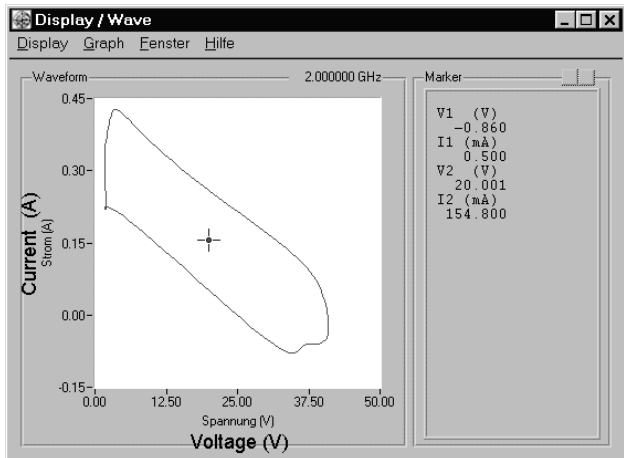


Fig. 5: Corresponding I-V trajectory for measurements shown in Fig. 4.

S-parameter measurements yield  $f_T$  values of 24 GHz and  $f_{max}$  values above 50 GHz for  $1 \times 3 \times 30 \mu\text{m}^2$  HV-HBTs with a collector doping of  $6 \times 10^{15} \text{ cm}^{-3}$ . The onset of Kirk effect is observed when the collector current density exceeds  $2 \times 10^4 \text{ A/cm}^2$ .

Fig. 4 shows results of on-wafer load-pull measurements of  $10 \times 3 \times 30 \mu\text{m}^2$  HV-HBTs with  $6 \times 10^{15} \text{ cm}^{-3}$  collector doping. At a bias voltage of 20 V this device delivers an output power  $P_{out}$  of more than 2 W with good power added efficiency (PAE) of 66%. Furthermore, one should emphasize that this is achieved at a load impedance above  $50 \Omega$  as visible from the location in the Smith chart shown in Fig. 4. This is more than one order of magnitude higher than for low-voltage HBTs of comparable output power and greatly improves combining efficiency for large power cells. Fig. 5 presents the corresponding I-V trajectory.

## CONCLUSIONS

Very promising results are obtained on special HBTs for high-voltage operation. Relatively small 10-finger HV-HBTs ( $10 \times 3 \times 30 \mu\text{m}^2$ ) operated at 20 V deliver 2.2 W of microwave power with a PAE of 66% at 2 GHz. Further improvement of the operating voltage and available output power can be expected after including electrical ballasting and a better thermal stabilization of the power cells.

## ACKNOWLEDGEMENTS

The authors would like to thank D. Rentner and K. Ickert for their expert technical assistance during wafer processing. Financial support by the Bundesministerium für Bildung und Forschung (BMBF) under contract 01BM050 is gratefully acknowledged.

## REFERENCES

- [1] D. Hill, T.S. Kim, IEEE Trans. on Microwave Theory and Techniques. 45 (1997) 2224.
- [2] M. Achouche, S. Kraus, T. Spitzbart, M. Rudolph, P. Kurpas, D. Rentner, F. Brunner, E. Richter, T. Bergunde, P. Heymann, P. Wolter, H. Wittrich, M. Weyers, J. Würfl, G. Tränkle Inst. Phys. Conf. Ser. 166 (1999) 297.